Aerosol Technology

Properties, Behavior, and Measurement of Airborne Particles

Second Edition

William C. Hinds
Department of Environmental Health Sciences
Center for Occupational and Environmental Health
UCLA School of Public Health
Los Angeles, California

1999

A WILEY-INTERSCIENCE PUBLICATION
JOHN WILEY & SONS, INC.
NEW YORK / CHICHESTER / WEINHEIM / BRISBANE / SINGAPORE / TORONTO

11 Respiratory Deposition

The hazard caused by inhaled particles depends on their chemical composition and on the site at which they deposit within the respiratory system. Thus, an understanding of how and where particles deposit in our lungs is necessary to evaluate properly the health hazards of aerosols. Such an understanding is also central to the effective administration of pharmaceutical aerosols by inhalation. Humans have evolved effective defense mechanisms against aerosol hazards, and we consider here the first line of defense: mechanisms that restrict access of particles the sensitive regions of the lungs.

The deposition of particles in the lungs relies on the same basic mechanisms that cause collection in a filter, but the relative importance of each mechanism is quite different. While filtration occurs in a fixed system at a steady flow rate, respiratory deposition occurs in a system of changing geometry, with a flow that changes with time and cycles in direction. This added complexity means that predicting deposition from basic theory is much more difficult, and we must rely to a greater extent on experimental data and empirically derived equations. In this chapter, we review the basic mechanisms of particle deposition as they apply to the respiratory system, the characteristics of particle deposition in the lungs, and the entry of particles into the mouth or nose during inhalation. To gain an understanding of these features, it is necessary to review first the characteristics of the human respiratory system.

11.1 THE RESPIRATORY SYSTEM

From the standpoint of respiratory deposition, the respiratory system can be divided into three regions, each covering several anatomical units. These regions differ markedly in structure, airflow patterns, function, retention time, and sensitivity to deposited particles. The first is the *head airways region*, which includes the nose, mouth, pharynx, and larynx. It is also called the extrathoracic or nasopharyngeal region. Inhaled air is warmed and humidified in this region. The second region is the *lung airways* or *tracheobronchial* region, which includes the airways from the trachea to the terminal bronchioles. This region resembles an inverted tree, with a single trunk, the trachea, subdividing into smaller and smaller branches. Finally, beyond the terminal bronchioles is the *pulmonary* or *alveolar* region, where gas exchange takes place.

The respiratory system of a normal adult processes 10–25 m^3 (12–30 kg) of air per day. The surface area for gas exchange is about 75 m^2, half the size of a singles

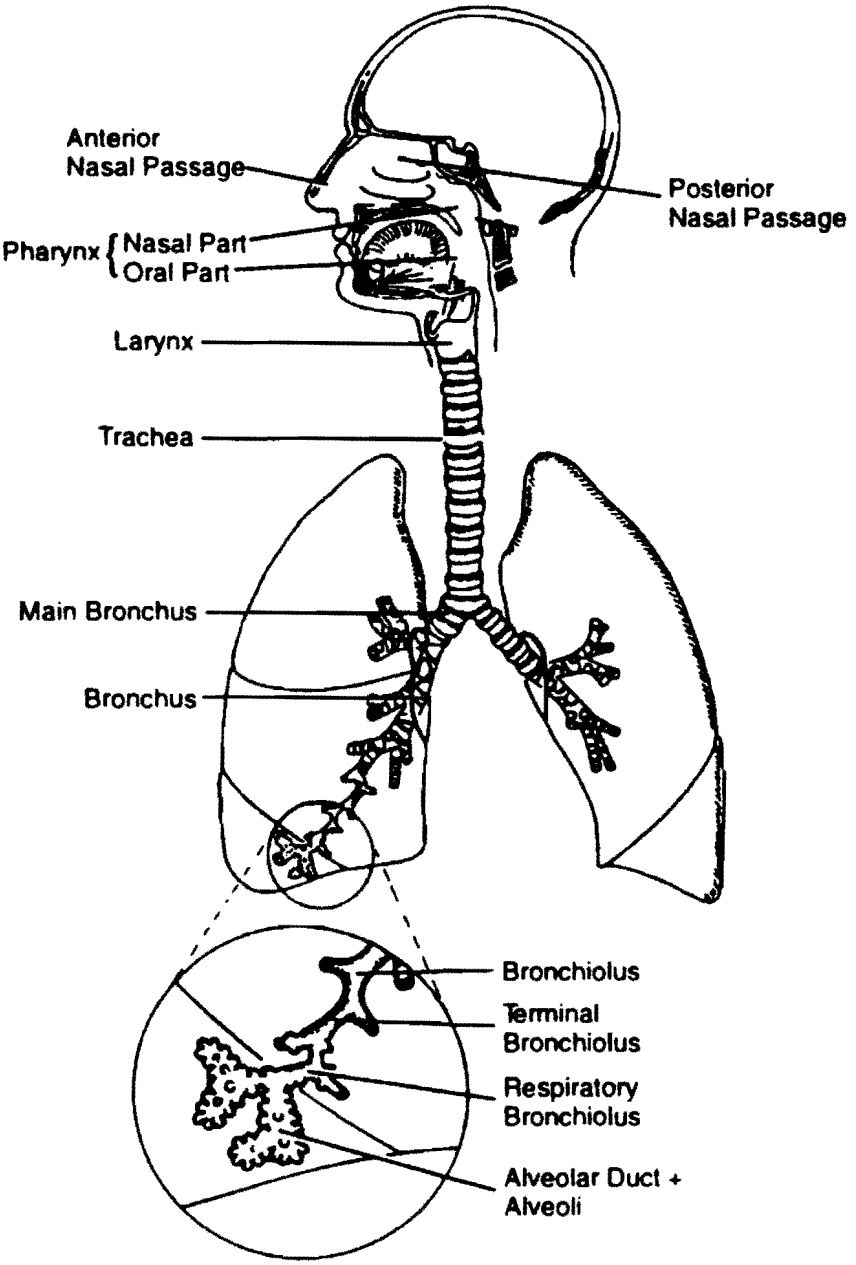

FIGURE 11.1 The respiratory system. Adapted from International Commission on Radiological Protection (1994).

tennis court, and is perfused with more than 2000 km of capillaries. Figure 11.1 shows the parts of the respiratory system. At rest, about 0.5 L of tidal air is inhaled and exhaled with each breath. During heavy work, the tidal volume may exceed three times this amount. A resting adult breathes about 12 times a minute, a rate that triples during heavy work. About 2.4 L of reserve air is not exhaled during normal breathing, but nearly half of this can be exhaled by forced exhalation. Inhaled air follows a flow path that goes through a sequence of 23 airway branchings as it

travels from the trachea to the alveolar surfaces. The first 16 branchings take place in the tracheobronchial region and the remainder in the gas exchange region.

Once deposited, particles are retained in the lung for varying times, depending on their physicochemical properties, their location within the lung, and the type of clearance mechanism involved. The airway surfaces of the first two respiratory regions, the head and lung airways, are covered with a layer of mucus that is slowly propelled by ciliary action to the pharynx, where it is subconsciously swallowed to the gastrointestinal tract. This mucociliary escalator transports particles deposited in the airways out of the respiratory system in a matter of hours. This clearance mechanism can be accelerated by low doses of irritating gases or aerosols, or it can be slowed by high doses of such materials or by overloading with particles. Because of its gas exchange function, the alveolar region does not have this protective mucus layer. Hence, insoluble particles deposited in this region are cleared very slowly, over a period of months or years. Dissolved particles pass through the thin alveolar membrane into the bloodstream. Solid particles may dissolve slowly or be engulfed by alveolar macrophages (phagocytic cells) and dissolved or transported to lymph nodes or the mucociliary escalator. Fibrogenic dusts, such as silica, interfere with this clearance mechanism and cause gradual scarring or fibrosis of the alveolar region.

Table 11.1 gives the characteristics of various parts of the lung. During inhalation at a steady rate of 3.6 m^3/hr [1 L/s], the velocity in the airways increases slightly until the air reaches the lobar bronchi. After that, the velocity decreases rapidly during the remaining 70 or 80 mm of transit. This rapid decrease in velocity is a result of the tremendous increase in the total airway cross-sectional area due to the large number of small airways. The total cross-sectional area of the airways expands by a factor of 250 from the lobar bronchi to the respiratory bronchioles, and velocity decreases by the same factor. In normal breathing, freshly inhaled air pushes the residual air ahead of it, so that the fresh air travels only as far as the alveolar ducts. Nevertheless, gas exchange takes place readily by diffusion of O_2 and CO_2 over the very short terminal distances (< 1 mm). In the trachea and main bronchi, the airflow can be turbulent at peak inspiratory and expiratory flow rates for the normal breathing cycle. The remaining airflow is laminar under normal conditions, but, because the airway sections are relatively short compared with their diameters (length $\approx 3\times$ diameter), the airflow in these smaller airways is not fully developed laminar flow. This further complicates mathematical analysis and modeling. The air velocities given in Table 11.1 are based on steady flow, whereas during actual breathing, the airflow rate is continuously changing and reverses direction twice each cycle.

11.2 DEPOSITION

Inhaled particles may deposit in the various regions of the respiratory system by the complex action of the five deposition mechanisms described in Section 9.3 or

TABLE 11.1 Characteristics of Selected Regions of the Lung[a]

Airway	Generation	Number per Generation	Diameter (mm)	Length (mm)	Total Cross Section (cm^2)	Velocity[a] (mm/s)	Residence Time[b] (ms)
Trachea	0	1	18	120	2.5	3900	30
Main bronchus	1	2	12	48	2.3	4300	11
Lobar bronchus	2	4	8.3	19	2.1	4600	4.1
Segmental bronchus	4	16	4.5	13	2.5	3900	3.2
Bronchi with cartilage in wall	8	260	1.9	6.4	6.9	1400	4.4
Terminal bronchus	11	2000	1.1	3.9	20	520	7.4
Bronchioles with muscles in wall	14	16,000	0.74	2.3	69	140	16
Terminal bronchiole	16	66,000	0.60	1.6	180	54	31
Respiratory bronchiole	18	0.26×10^6	0.50	1.2	530	19	60
Alveolar duct	21	2×10^6	0.43	0.7	3200	3.2	210
Alveolar sac	23	8×10^6	0.41	0.5	72,000	0.9	550
Alveoli		300×10^6	0.28	0.2			

[a]Based on Weibel's model A; regular dichotomy average adult lung with volume. 0.0048 m^3 [4800 cm^3] at about three-fourths maximal inflation. Table adapted from Lippmann (1995).
[b]At a flow rate of 3.6 m^3/hr [1.0 L/s].

they may be exhaled. The most important of these mechanisms are impaction, settling, and diffusion; interception and electrostatic deposition are only important in certain situations. Particles that contact the airway walls deposit there and are not reentrained. The extent and location of particle deposition depend on particle size, density, and shape; airway geometry; and the individual's breathing pattern.

To describe aerosol deposition within the respiratory system analytically requires a complete solution of the constantly changing hydrodynamic flow field in the respiratory airways and the superposition of particle motion on that flow field. Currently, this is not possible; however, an understanding of the factors involved can be gained by examining the specific mechanisms that cause individual particles to deposit at different locations in the respiratory system. Understanding these mechanisms permits insight into the complex relationship between respiratory deposition and particle size, breathing frequency, flow rate, and tidal volume. The discussion that follows applies to healthy adults. Deposition characteristics may be quite different for others, such as children or people with respiratory disease.

During inhalation, the incoming air must negotiate a series of direction changes as it flows from the nose or mouth down through the branching airway system to the alveolar region. Each time the air changes direction, the suspended particles continue a short distance in their original direction because of their inertia. The net result is that some particles near the airway surfaces deposit there by *inertial impaction.* The effectiveness of this mechanism depends on the particle stopping distance at the airway velocity, which is comparatively low. Consequently, this mechanism is limited to the deposition of large particles that happen to be close to the airway walls. Nonetheless, the mechanism typically causes most aerosol deposition on a mass basis. The greatest deposition by impaction typically occurs at or near the first carina, the dividing point at the tracheal bifurcation, and to a lesser degree at other bifurcations. This is because the streamlines bend most sharply at bifurcations and pass close to the carina. Table 11.2 gives the ratios of particle stopping distances to airway dimensions at velocities associated with a steady inhalation of 3.6 m^3/hr [1.0 L/s] for selected airways. The probability of deposition by impaction depends on this ratio and is highest in the bronchial region.

While impaction is of primary concern in the large airways, *settling* is most important in the smaller airways and the alveolar region, where flow velocities are low and airway dimensions are small. Sedimentation has its maximum removal effect in horizontally oriented airways. Table 11.2 gives the ratio of the settling distance (terminal settling velocity × residence time in each airway, at a steady flow of 3.6 m^3/hr [1.0 L/s]) to the airway diameter. As can be seen, this mechanism is most important in the distal airways (those farthest from the trachea). Hygroscopic particles grow as they pass through the water-saturated airways, and this increase in size favors deposition by settling and impaction in the distal airways.

The *Brownian motion* of submicrometer-sized particles leads to an increased likelihood that they will deposit on airway walls, especially in the smaller airways, where distances are short and residence times comparatively long. Table 11.2 includes the ratio of the root-mean-square displacement during residence in selected airways to the airway diameter. This ratio determines the relative likelihood of depo-

TABLE 11.2 Relative Importance of Settling, Impaction, and Diffusion Mechanisms for Deposition of Standard Density Particles in Selected Regions of the Lung

	Stopping Distance[a]			Settling Distance[b]			Rms Displacement[c]		
	Airway Diameter (%)			Airway Diameter (%)			Airway Diameter (%)		
Airway	0.1 μm	1 μm	10 μm	0.1 μm	1 μm	10 μm	0.1 μm	1 μm	10 μm
Trachea	0	0.08	6.8	0	0	0.52	0.04	0.01	0
Main bronchus	0	0.13	10.9	0	0	0.41	0.03	0.01	0
Segmental bronchus	0	0.31	27.2	0	0	0.22	0.05	0.01	0
Terminal bronchus	0	0.17	14.9	0	0.02	2.1	0.29	0.06	0.02
Terminal bronchiole	0	0.03	2.8	0	0.18	15.6	1.1	0.22	0.06
Alveolar duct	0	0	0.23	0.04	1.7	150	3.9	0.79	0.23
Alveolar sac	0	0	0.07	0.12	4.7	410	6.7	1.3	0.40

[a]Stopping distance at airway velocity for a steady flow of 3.6 m^3/hr [1.0 L/s].
[b]Settling distance = settling velocity × residence time in each airway at a steady flow of 3.6 m^3/hr [1.0 L/s].
[c]Rms displacement during residence time in each airway at a steady flow of 3.6 m^3/hr [1.0 L/s].

sition by diffusion. The airway and flow conditions that favor settling—that is, a small diameter and a long residence time—also favor diffusion. Diffusion is the predominant deposition mechanism for particles less than 0.5 μm in diameter and is governed by geometric, rather than aerodynamic, particle size.

Interception is the process by which a particle, without deviating from its gas streamline, contacts the airway surface because of its physical size. The likelihood of interception depends on the proximity of the gas streamline to the airway surface and on the ratio of particle size to airway diameter, which is usually small even in the smallest airways. One exception to this is the case of long fibers, which are large in one dimension, but have small aerodynamic diameters. Long fibers can readily traverse the tortuous path to the small airways, where they have a high likelihood of interceptive deposition.

Highly charged particles are attracted to airway surfaces by the *electrostatic* image charge that the particle induces in the airway surface by its presence. Unipolar charged aerosols with high number concentrations are also deposited because their mutual repulsion drives particles away from each other and toward the airway walls.

Total deposition—the combined deposition of particles in all regions of the respiratory system—is usually determined experimentally by measuring the concentration of inhaled and exhaled monodisperse test aerosols under controlled conditions. A person's breathing frequency, the volume of air he or she inhales, and the length of the pause between inhalation and exhalation all affect the deposition of inhaled particles. For particles with an aerodynamic diameter larger than 0.5 μm, the lower the breathing frequency (number of breaths per minute), the greater the fractional deposition, because there is more time for gravity settling. For particles larger than about 1 μm, deposition increases with the average airflow rate, because of the velocity-dependent mechanism of inertial impaction. A pause in the breathing cycle between inhalation and exhalation increases the deposition of particles for all size ranges, particularly for larger particles and longer pauses. Figure 11.2 shows the total deposition for a wide range of particle sizes, based on the International Commission on Radiological Protection (ICRP) deposition model. (See Section 11.3.)

Although most experimental studies have measured only total deposition, *regional deposition* within the lung is important for assessing the potential hazard of inhaled particles. To evaluate the hazard, the effective dose at the critical site within the lung where injury is initiated must be known. The deposition in any respiratory region depends on deposition in preceding regions, as well as on the deposition efficiency for the region. Generally, deposition in the head and tracheobronchial regions serve to protect the alveolar region of the lungs from irritating or harmful particles. Figure 11.3 shows the total and regional deposition predicted by the ICRP model (see Section 11.3) as a function of particle size, for particles from 0.001 to 100 μm.

Deposition of particles in the *head airways region* is highly variable and depends on several factors, including whether mouth or nose breathing is used, flow rates, and particle size. Air taken in through the nose is warmed and humidified while

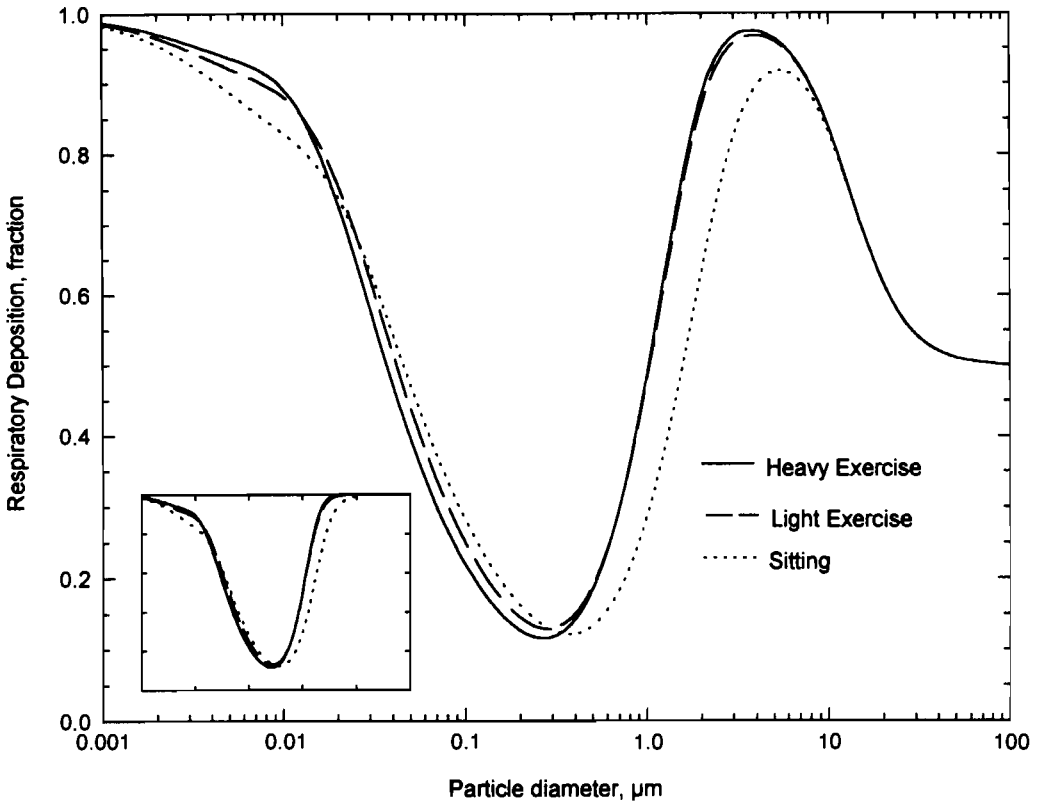

FIGURE 11.2 Predicted total respiratory deposition at three levels of exercise based on ICRP deposition model. Average data for males and females. Inset does not include the effect of inhalability.

passing around shelf-like turbinates in the nasal passage. The largest particles are removed by settling and by impaction on nasal hairs and at bends in the airflow path. Those particles deposited on the ciliated surfaces of the nasal cavity are cleared to the pharynx and swallowed. For mouth breathing at an inspiratory flow rate of 1.8 m^3/hr [30 L/min], approximately 20% of 5-μm aerodynamic diameter particles and 70% of 10-μm particles (aerodynamic diameter) are deposited before the inhaled air reaches the larynx. Under conditions of light exercise and nose breathing, 80% of inhaled 5-μm particles and 95% of inhaled 10-μm particles are trapped in the nose. For both mouth and nose breathing, deposition in the head region increases when average inspiratory flow rate increases. Ultrafine particles less than 0.01 μm have significant deposition in the head airways due to their high diffusion coefficients.

At an average inspiratory flow rate of 1.2 m^3/hr [20 L/min] or greater, impaction is the dominant mechanism for the deposition of particles larger than 3 μm in the *tracheobronchial region.* For particles 0.5–3 μm or flow rates less than 1.2 m^3/hr [20 L/min], settling is the predominant mechanism of deposition, although overall tracheobronchial deposition for particles in this size range is quite small. For conditions of light exercise, particles with aerodynamic diameters of 5 and 10 μm that reach the tracheobronchial region are deposited there with approximately 35 and

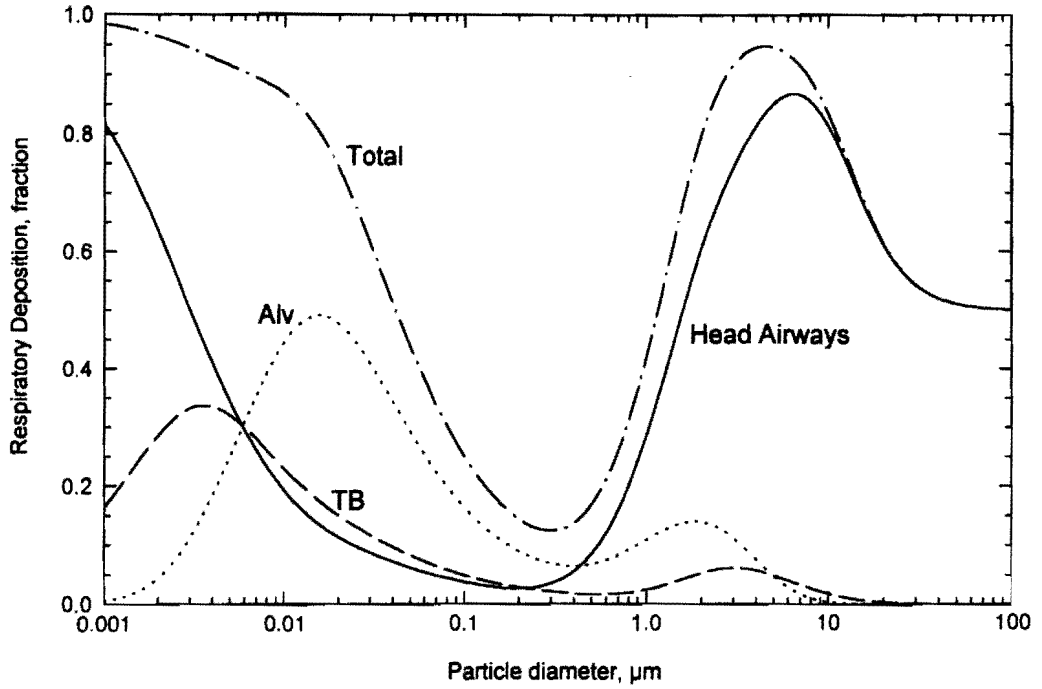

FIGURE 11.3 Predicted total and regional deposition for light exercise (nose breathing) based on ICRP deposition model. Average data for males and females.

90% efficiency, respectively. These efficiencies increase significantly with increased breathing rate. During exercise, there can be significant mixing of inhaled air with the reserve air in the first few sections of the tracheobronchial region due to turbulence in these airways. This mixing transfers particles from tidal to reserve air facilitating subsequent deposition of submicrometer-sized particles in the alveolar region. Ultrafine particles, especially those less than 0.01 μm, have enhanced deposition in the tracheobronchial region due to their rapid Brownian motion.

Alveolar deposition is usually expressed as the fraction of the inhaled particles traversing the head airways region that ultimately deposit in the alveolar region. Because of size-selective particle deposition in the tracheobronchial region, particles larger than 10 μm generally do not reach the alveolar region, and particles in the 2–10 μm range reach the alveolar region in attenuated numbers. Deposition in the alveolar region depends on particle size, breathing frequency, and tidal volume. As shown in Figure 11.3, alveolar deposition is reduced whenever tracheobronchial and head airway deposition is high. Thus, these rapidly cleared regions serve to protect the more vulnerable alveolar region.

Inhaled air penetrates the alveolar region with a thin parabolic velocity profile along the axis of each airway. With normal breathing, the apices of the parabolas do not enter the alveoli and gas exchange takes place by molecular diffusion over the last millimeter. At the low air velocities and small dimensions in this region, gas diffusion is a faster transport mechanism than flow. Inhaled submicrometer-sized particles are not directly deposited in the alveolar region, because their settling is too low and their diffusion is orders of magnitude slower than that of gas molecules.

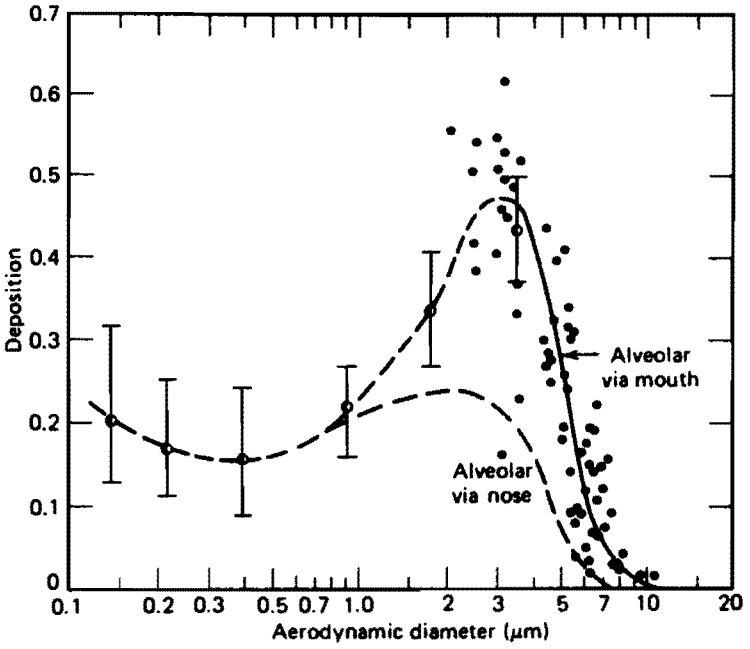

FIGURE 11.4 Experimental data for deposition in the alveolar region. Deposition is expressed as a fraction of mouthpiece inhalation versus aerodynamic diameter (geometric diameter used below 0.5 μm). Reprinted with permission from Lippmann (1977).

The deposition of these particles is controlled by their transfer from the inhaled air to the reserve air in the tracheobronchial region, followed by settling from the trapped reserve air in the alveolar region. Consequently, the rate of alveolar deposition for particles 0.1–1 μm is about 10–20% and is approximately independent of the particle size. As shown in Fig. 11.4, the particle size having the greatest deposition in the alveolar region during mouth breathing is about 3 μm, with approximately 50% of these particles being captured in the alveolar region. During nose breathing, the size for maximum alveolar deposition is reduced to about 2.0 μm, with about 10–20% of these particles being retained.

11.3 DEPOSITION MODELS

Many mathematical models for predicting total and regional deposition have been developed. [See Lippmann (1995).] Two advanced and widely used models are those of the International Commission on Radiological Protection (ICRP, 1994) and the National Council on Radiation Protection and Measurement (NCRP, 1997). These models were developed to estimate the dose to organs and tissue resulting from the inhalation of radioactive particles by typical males and females, both adults and children. The models are based on experimental data, theory, and an earlier ICRP model developed in the 1960s. Each estimates regional and total deposition over a wide range of particle sizes, essentially all aerosol particle sizes, and the full

range of breathing conditions. While they apply to typical adults and children, there is large intersubject variability for respiratory deposition, and individuals may have very different deposition patterns. Each model is sufficiently complicated that a computer is required to do the calculations. In addition to modeling deposition, they model clearance, give transport rates between regions and the dose to tissues, including the thoracic lymph nodes.

The two models differ in their approach to calculating regional deposition. The ICRP model uses empirical equations based on experimental data and theory to characterize deposition by settling, inertia, and diffusion in five regions of the respiratory system: the nose and mouth, throat and larynx, upper airways (bronchi), lower airways (bronchioles), and alveolar. The NCRP model uses an empirical equation for deposition in the nose and throat; deposition in the remainder of the respiratory system is calculated using a detailed table of airway geometry for each branching generation and the alveolar region. Deposition is calculated for each generation by aerosol mechanics equations similar to those given in Chapters 3, 5, and 7 for settling, inertia, and diffusion. Data and equations are given by Yeh and Schum (1980) and Yeh et al. (1996). Both models give similar predictions for total deposition and that in the head airways, but differ in the proportioning of deposition between the tracheobronchial region and the alveolar region, especially for particles less than 0.1 μm. However, the differences in predicted deposition by these models are small compared to the differences in deposition among normal individuals.

Figure 11.2 shows the total deposition predicted by the ICRP deposition model (International Commission on Radiological Protection, 1994) for adults at three levels of exercise: sitting, light exercise, and heavy exercise. Calculations were done for spheres of standard density at standard conditions. Results for males and females were averaged. Respiratory parameters used in the model's calculations are given in Table 11.3. Figure 11.2 includes the effect of inhalability, or the fraction of ambient particles of a given size that can enter the mouth or nose. (See Section 11.4.)

TABLE 11.3 Respiratory Parameters Used in the ICRP Model

	Functional Reserve Capacity, FRC (L)	Breathing Rate (m^3/hr)	Breathing Frequency (breaths/min)	Tidal Volume (L)
Female				
Sitting	2.68	0.39	14	0.46
Light Exercise	2.68	1.25	21	0.99
Heavy Exercise	2.68	2.7	33	1.36
Male				
Sitting	3.30	0.54	12	0.75
Light Exercise	3.30	1.5	20	1.25
Heavy Exercise	3.30	3	26	1.92

The inset in the figure shows the total deposition as a fraction of what is inhaled. A comparison of the inset and the main figure reveals that the inhalability effect is quite significant for particles larger than a few micrometers. The figure shows that different levels of exercise have relatively little effect on total deposition, except that sitting yields lower deposition than exercising does for particles in the 1–5-μm range. The figure also shows a pronounced minimum at about 0.3 μm, a size that is too small for significant deposition by inertia and settling and too large for significant deposition by diffusion.

Figure 11.3 shows total and regional deposition for adults engaged in light work, according to the ICRP model. For particles larger than 1 μm, total deposition is dominated by deposition in the head airways. Elsewhere, total deposition reflects deposition in two or more regions. Deposition in any region is affected by deposition in the preceding regions. Thus, only particles that are inhaled can be deposited in the head airways, and only particles passing beyond the head airway region can be deposited in the tracheobronchial region. Deposition in the alveolar region is reduced by deposition in the previous two regions. During exhalation flow direction reverses and deposition in each region is decreased due to the deposition in the preceding deeper-lying regions. Deposition in the head airways increases for particles less than 0.01 μm due to diffusion, especially in the nose. This causes deposition in the lung airways and alveolar regions to drop off for the smallest particles.

The following simplified equations were fitted to the ICRP model for monodisperse spheres of standard density at standard conditions. Data for males and females at three exercise levels were averaged. Deposition fractions predicted by these equations agree with the ICRP model within ±0.03 over the size range of 0.001 to 100 μm. In Eqs. 11.1–11.5, d_p is particle size in μm. The deposition fraction for the head airways DF_{HA} is

$$DF_{HA} = IF\left(\frac{1}{1 + \exp(6.84 + 1.183 \ln d_p)} + \frac{1}{1 + \exp(0.924 - 1.885 \ln d_p)}\right) \quad (11.1)$$

where IF is the inhalable fraction (see next section). Inhalable fraction as used by the ICRP model is given by

$$IF = 1 - 0.5\left(1 - \frac{1}{1 + 0.00076 d_p^{2.8}}\right) \quad (11.2)$$

The deposition fraction for the tracheobronchial region DF_{TB} is

$$DF_{TB} = \left(\frac{0.00352}{d_p}\right)[\exp(-0.234(\ln d_p + 3.40)^2) + 63.9 \exp(-0.819(\ln d_p - 1.61)^2)] \quad (11.3)$$

The deposition fraction for the alveolar region DF_{AL} is

$$\mathrm{DF_{AL}} = \left(\frac{0.0155}{d_p}\right)[\exp(-0.416(\ln d_p + 2.84)^2) + 19.11\exp(-0.482(\ln d_p - 1.362)^2)] \tag{11.4}$$

Although IF does not appear explicitly in Eqs. 11.3 and 11.4, they were fitted to data that included the effect of inhalability. The total deposition DF is the sum of the regional depositions, or

$$\mathrm{DF} = \mathrm{IF}\left(0.0587 + \frac{0.911}{1 + \exp(4.77 + 1.485\ln d_p)} + \frac{0.943}{1 + \exp(0.508 - 2.58\ln d_p)}\right) \tag{11.5}$$

Figures 11.2 and 11.3 and Eqs. 11.1–11.5 are for spheres of standard density, but can be applied to other particles by using the aerodynamic diameter for particles larger than 0.5 μm and the physical diameter or equivalent volume diameter for particles less than 0.5 μm. For spheres, $d_a = d_p(\rho_p/\rho_o)^{1/2}$; for nonspheres, see Eq. 3.27.

The mass of a given particle size deposited in the respiratory system per minute M_{dep} is

$$M_{\mathrm{dep}} = \frac{\pi}{6} N\rho_p d_p^3 V_m(\mathrm{DF}) \tag{11.6}$$

where N is the number concentration of particles of diameter d_p and density ρ_p, V_m is the minute volume or volume inhaled in 1 min, and DF is the total deposition fraction for particle size d_p, Eq. 11.5. For regional deposition, DF is replaced by the appropriate regional deposition fraction, Eqs. 11.1, 11.3, or 11.4.

EXAMPLE

What fraction of *inhaled* 5-μm particles will deposit in the head airway region? Asume standard density and an adult engaged in light work.

$$\mathrm{DF_{HA}} = 1\left(\frac{1}{1 + \exp(6.84 + 1.183\ln(5.0))} + \frac{1}{1 + \exp(0.924 - 1.885\ln(5.0))}\right)$$

$$= 1(0.00016 + 0.892) = 0.89.$$

11.4 INHALABILITY OF PARTICLES

The entry of particles into the mouth or nose can be thought of as a sampling process—one that includes elements from isokinetic and still-air sampling. Unlike thin-

wall sampling probes, the human head is a *blunt sampler* with a complex geometry. Theoretical approaches and experimental results for blunt samplers have been reviewed by Vincent (1989). As air approaches a blunt sampler, the streamlines display two kinds of distortion: A larger scale divergence occurs as the air flows around the blunt object, and a smaller scale convergence occurs near the inlet. This motion is considerably more complicated than that for isokinetic sampling, and there seems to be no condition that ensures perfect sampling for all particle sizes.

The efficiency of entry of particles into the nose or mouth can be characterized by the *aspiration efficiency, inhalability, or inhalable fraction* (*IF*), the fraction of particles originally in the volume of air inhaled that enters the nose or mouth. The inhalable fraction is usually less than one, but can be greater than one under some conditions. It depends on particle aerodynamic diameter and the external wind velocity and direction. Inhalability fraction is determined experimentally, typically in a large, low-velocity wind tunnel with a full-size, full-torso mannequin connected to a mechanical breathing machine. A uniform concentration of dust flows past the mannequin. A series of test dusts with narrow size distributions is used. Together, these dusts cover the range of 5 to 100 μm or more in aerodynamic diameter. Air velocities up to 4 m/s are used to simulate indoor environments and up to 10 m/s to simulate outdoor environments. The mannequin can be positioned at any angle to the wind direction or continuously rotated. Inhaled dust is collected by a sampling filter immediately inside the mouth or nose. Reference samples are usually taken by isokinetic samplers located near the mannequin's head. For a given condition and particle size, inhalable fraction is the ratio of the concentration calculated on the basis of the collected mass and sample volume for the mouth (or nose) filter to that calculated for the isokinetic samplers.

Inhalable fraction data are usually presented as "orientation averaged," meaning that all orientations with respect to the wind direction are equally represented. Orientation-averaged mouth inhalability data are summarized in Figure 11.5, which includes the ACGIH inhalable particulate matter (IPM) sampling criterion (ACGIH, 1996). The curve defines the desired sampling performance of an IPM sampler in terms of the fractional collection for particles up to 100 μm. This criterion is the same as that proposed by the International Standards Organization (ISO 7708) and the Comité Européen de Normalisation (CEN EN481). The equation for the inhalable fraction and inhalable fraction sampling criterion IF(d_a) is

$$\mathrm{IF}(d_a) = 0.5(1 + \exp(-0.06\, d_a)) \quad \text{for } U_0 < 4 \text{ m/s} \tag{11.7}$$

where d_a is the aerodynamic diameter in μm. Vincent et al. (1990) give the following expression for inhalability when the ambient air velocity U_0 is greater than 4 m/s.

$$\mathrm{IF}(d_a, U_0) = 0.5(1 + \exp(-0.06 d_a)) + 10^{-5} U_0^{2.75} \exp(0.055\, d_a) \tag{11.8}$$

where d_a is in μm ($d_a < 100$ μm) and U_0 is in m/s. Equation 11.8 reduces to Eq. 11.7 within ±5% for $d_a < 30$ μm and $U_0 < 10$ m/s and for $d_a < 100$ μm and $U_0 < 3$ m/s. There are fewer data for nasal inhalability IF_N which can be approximated by

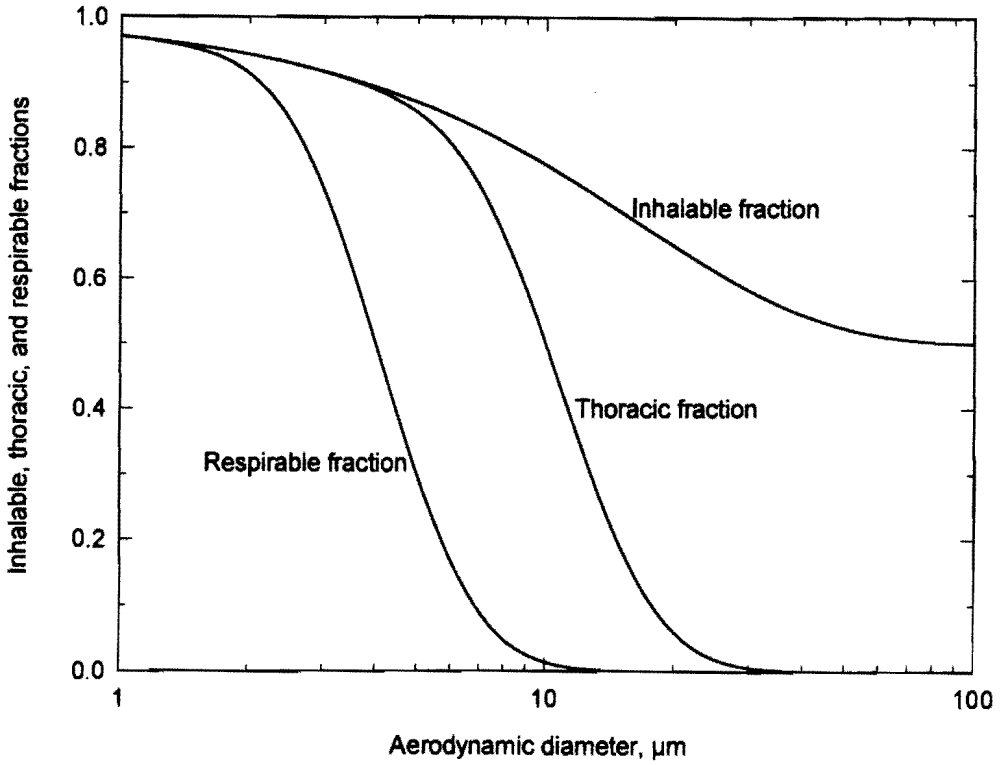

FIGURE 11.5 ACGIH sampling criteria for inhalable, thoracic, and respirable fractions.

$$\mathrm{IF}_N(d_a) = 0.035 + 0.965 \exp(-0.000113 d_a^{2.74}) \tag{11.9}$$

where d_a is the aerodynamic diameter in μm (Hinds et al., 1998).

EXAMPLE

What is the inhalable fraction for 18-μm particles of standard density? Assume that $U_0 < 4$ m/s.

By Eq. 11.7,

$$\mathrm{IF} = 0.5(1 + \exp(-0.06 \times 18)) = 0.67$$

The performance of *inhalable samplers* is usually evaluated in a low-velocity wind tunnel similar to that described for the evaluation of inhalability. The samplers are tested one particle size at a time. A sampler's performance can be expressed in one of two ways: first as the ratio of the concentration measured by the sampler to the true ambient air concentration as measured by the isokinetic samplers or, alternatively, as the ratio of the concentration measured by the sampler to the inhalable concentration. The latter can be determined using a mannequin, or by

isokinetic samplers and calculation using the inhalable fraction curve. The first method provides an absolute measure of the ability of the sampler to sample accurately the inhalable fraction of particles of a given size in the ambient environment. The results obtained can be compared directly to the inhalable sampling-criteria curve. The second method provides a relative measure of how well the sampler conforms to the inhalable sampling criterion.

More than a dozen area and personal samplers have been designed to meet the inhalable sampling criterion. An area sampler developed by Mark et al. (1985) conforms well to the inhalable sampling criteria. The device has a cylindrical rotating (2 rpm) sampling head 50 mm in diameter and 60 mm high with a 3 × 15-mm oval inlet on the side. It is battery powered and samples at 0.18 m^3/hr [3 L/min] onto a 37-mm filter mounted in a weighable cassette.

The most commonly used personal inhalable sampler is the Institute for Occupational Medicine (IOM) personal sampler described by Mark and Vincent (1986). The device, shown in Fig. 11.6, has a cylindrical body 37 mm in diameter with a protruding inlet 15 mm in diameter. It is attached to a worker's lapel, so that the inlet is always facing forward. The filter and its lightweight cassette are weighed together so that any particles that deposit in the inlet are included in the sample. The device shows good agreement with the inhalable sampling criterion for $U_0 \leq 1.0$ m/s. A conductive plastic version of this sampler is manufactured by SKC, Inc., of Eighty Four, PA.

Kenny et al. (1997) evaluated the performance of eight designs of personal inhalable samplers. Five performed satisfactorily at 0.5 m/s, two at 1 m/s, and none

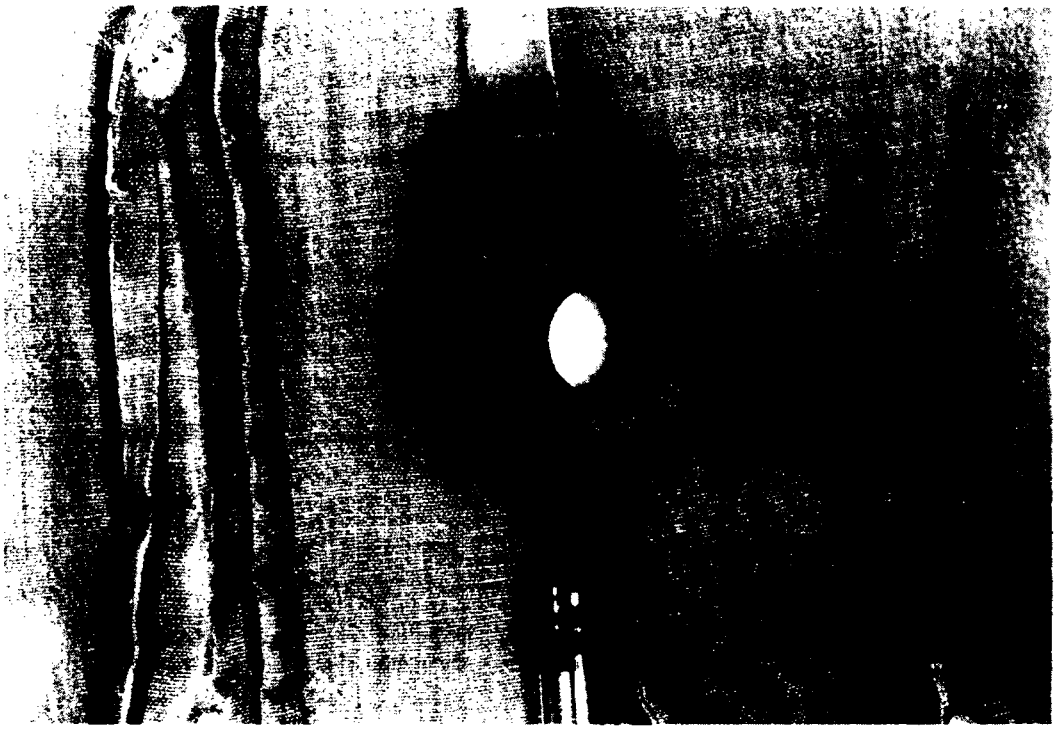

FIGURE 11.6 IOM-type personal inhalable aerosol sampler.

TABLE 11.4 Comparison of Performance of IOM Sampler with that of Inhalable 37-mm in-line Personal Sampler[a]

Aerosol	IOM Concentration / 37-mm Concentration
Mineral dust, flour	2.5
Oil mist, paint spray	2.0
Smelter, foundry	1.5
Smoke, fume, welding	1.0

[a]Adapted from Werner et al. (1996).

at 4 m/s. The commonly used in-line 37-mm plastic filter cassette undersamples particles larger than 30 μm in aerodynamic diameter. The open-face version undersamples particles larger than 30 μm for $U_0 \leq 1.0$ m/s and oversamples all sizes at 4 m/s. Results of side-by-side simultaneous sampling with the IOM personal sampler and 37-mm in-line samplers are summarized in Table 11.4. Inhalable particle samplers are reviewed by Hinds (1999).

11.5 RESPIRABLE AND OTHER SIZE-SELECTIVE SAMPLING

An understanding of regional deposition has spurred the development of health-based, particle size-selective sampling—that is, sampling a subset of the airborne particles on the basis of their aerodynamic size. The subset is chosen to select those particles that can reach a particular region of the respiratory system and potentially deposit there. Other sizes are excluded from the sample. In the field of occupational health, examples are inhalable, thoracic, and respirable sampling, as well as cotton dust sampling. In the field of ambient air quality, examples are PM-10 and PM-2.5.

Respirable sampling was first used in the 1950s to assess occupational exposure to silica dust. For that purpose, we need information on the amount of dust that can deposit at the site of toxic action, the alveolar region of the lungs. Because of the size-selective characteristics of the human respiratory system, particles larger than a certain size are unable to reach the alveolar region and therefore can be considered nonhazardous with respect to alveolar injury. To estimate the potential hazard of silica or other dusts that have their site of toxic action in the alveolar region, we must exclude these nonhazardous particles from our assessment.

Historically, respirable sampling was performed for harmful mineral dusts by using microscopic particle counting. The hazard was assessed by number concentration (dust counting) instead of mass concentration, because the former correlated with the prevalence and extent of respiratory disease observed in miners. The reason mass concentration does not correlate with disease can be seen in Fig. 11.7. More than 60% of the mass of a typical mine aerosol is contributed by particles that are nonrespirable, that is they are too large to reach the alveolar region, whereas about 98% of the *number* of particles can reach the alveolar region. Thus, number concentration more closely reflects the hazard in this situation.

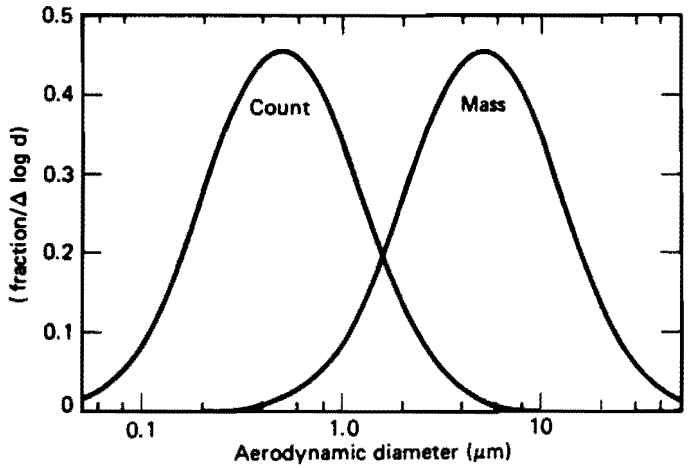

FIGURE 11.7 Typical count and mass distributions for mine dust.

Respirable sampling uses a mechanical device upstream of the sampling filter to aerodynamically remove those particles which are "nonrespirable"—that is, which are unable to reach the alveolar region. The *respirable mass* of an airborne dust is estimated by gravimetric analysis of that portion that passes through the device, or precollector. This approach is called respirable sampling, respirable mass sampling, or size-selective sampling. Unfortunately, the particle size cutoff that separates respirable from nonrespirable particles is not sharp, but extends gradually over the range of 2–10 μm, as shown in Fig 11.5. Respirable sampling is simpler, quicker, and more accurate than counting dust particles.

The *respirable fraction*, RF, is defined by the American Conference of Governmental Industrial Hygienists (ACGIH) particle size-selective sampling criteria as

$$\mathrm{RF} = (\mathrm{IF})(1 - F(x)) \tag{11.10}$$

where IF is the inhalable fraction given by Eq. 11.7 and $F(x)$ is the cumulative fraction for a standardized normal variable x.

$$x = 2.466 \ln(d_a) - 3.568 \tag{11.11}$$

in which d_a is aerodynamic diameter in μm.

The quantity x is the number of standard deviations d_a is from the mean of 4.25 μm and $1 - F(x)$ is the fraction of *inhaled* particles that can reach the alveolar region. $F(x)$ can be approximated by

$$F(x) = 0.5(1 - 0.1969x + 0.1152x^2 - 0.0003x^3 + 0.0195x^4)^{-4} \quad \text{for } x \le 0$$

$$F(x) = 1 - 0.5(1 + 0.1969x + 0.1152x^2 + 0.0003x^3 + 0.0195x^4)^{-4} \quad \text{for } x > 0 \tag{11.12}$$

where x is given by Eq. 11.11. This approximation, together with Eqs 11.10 and 11.11, predicts the respirable fraction to within 1% of the correct value, for all values

TABLE 11.5 Inhalable, Thoracic, and Respirable Fractions[a]

Aerodynamic Diameter (μm)	Inhalable Fraction	Thoracic Fraction	Respirable Fraction
0	1.00	1.00	1.00
1	0.97	0.97	0.97
2	0.94	0.94	0.91
3	0.92	0.92	0.74
4	0.89	0.89	0.50
5	0.87	0.85	0.30
6	0.85	0.81	0.17
8	0.81	0.67	0.05
10	0.77	0.50	0.01
15	0.70	0.19	0.00
20	0.65	0.06	0.00
25	0.61	0.02	0.00
30	0.58	0.01	0.00
35	0.56	0.00	0.00
40	0.55	0.00	0.00
50	0.52	0.00	0.00
60	0.51	0.00	0.00
80	0.50	0.00	0.00
100	0.50	0.00	0.00

[a]ACGIH (1997).

of the respirable fraction greater than 0.005. A simpler approximation permits the direct calculation of RF in terms of IF and d_a,

$$\mathrm{RF} = (\mathrm{IF})(1 - \exp(-\exp(2.54 - 0.681\, d_a))) \tag{11.13}$$

The respirable fraction calculated by Eq. 11.13 differs from that calculated by Eqs. 11.10–11.12 by less than 0.007 for d_a from 0 to 100 μm. Table 11.5 and Figure 11.5 give values of inhalable, thoracic, and respirable fractions, as defined by the ACGIH (ACGIH, 1997). This definition of respirable fraction agrees with the equivalent ISO and CEN protocols. The respirable fraction is the fraction *passing through* or penetrating a respirable precollector, so the collection efficiency of the precollector for a particular particle size $\mathrm{CE}_R(d_a)$ is

$$\mathrm{CE}_R(d_a) = 1 - \mathrm{RF}(d_a) \tag{11.14}$$

Figure 11.8 compares the respirable fraction criterion with experimentally determined alveolar deposition curves. It should be borne in mind that the criterion attempts to define those particles that *reach* the alveolar region, whereas the deposition curves define those particles that *reach and are deposited in* the alveolar region. A better way to think about the function of a precollector is that it excludes particles from the sample in the same way that the airways of the respiratory system exclude particles from, or prevent particles from *reaching*, the alveolar region.

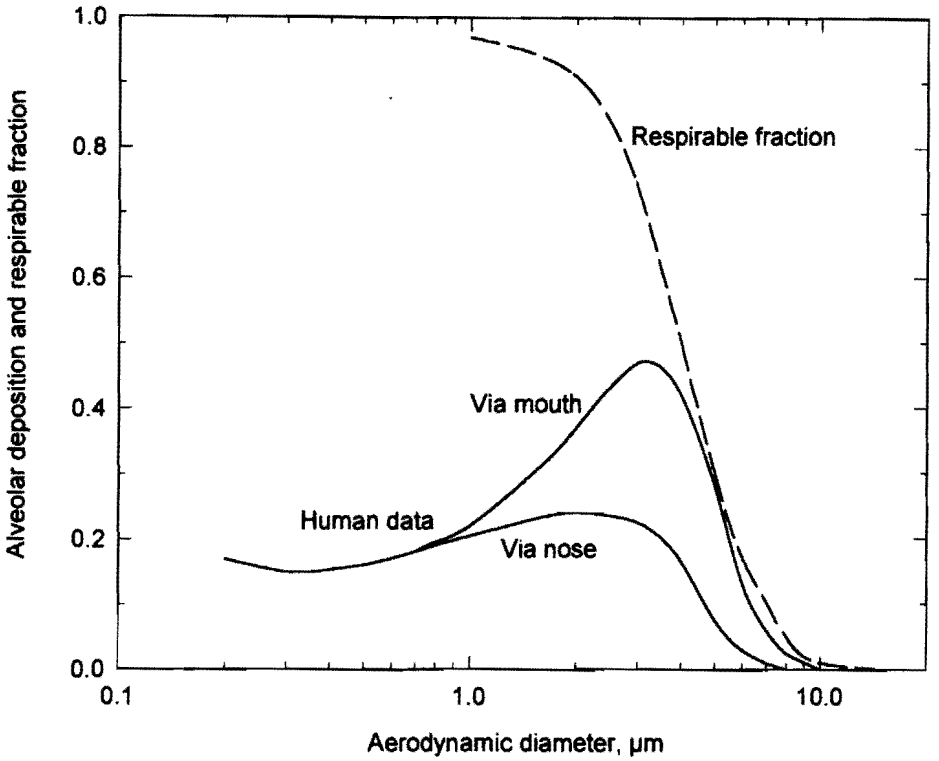

FIGURE 11.8 Comparison of experimental measurements of alveolar deposition (median values) and ACGIH respirable fraction criterion. Human data from Lippmann (1977).

It is recognized that the sampling filter will collect 100% of nonexcluded particles, whereas the alveolar region collects only about 20–40% of these nonexcluded particles, and exposure standards for respirable dust have been set accordingly. The criterion corresponds closely to the mouth-breathing alveolar deposition curve (Fig. 11.8), down to about 4 μm. Respirable sampling would, however, collect more particles greater than 4 μm than are likely to reach the alveolar region of a typical nose-breathing person. The use of respirable mass sampling is relevant only to dusts that have their site of toxic action or are absorbed in the alveolar region of the lung. In the United States, respirable dust standards exist for occupational exposure to cadmium, silica, coal, talc, and other mineral dusts. Nonrespirable particles of heavy metals or pesticides may not be damaging to the alveolar region of the lungs, but can be inhaled and cause serious injury elsewhere in the body.

The most widely used technique for respirable sampling is to use a cyclone for the precollector and a high-efficiency filter for the second-stage collector. Other, less common, approaches use horizontal elutriators, centrifugal inlets, specially designed impactors, open-cell foam, and large-pore capillary-pore-membrane filters as the precollector stage. The characteristics of some respirable precollectors are summarized in Table 11.6 and in Lippmann (1995).

In the United States, the most common precollector is the 10-mm nylon cyclone shown in Fig. 11.9. The dusty air is drawn into the cyclone through an inlet that is tangential to the cylindrical part of the cyclone. The inlet geometry causes the air

TABLE 11.6 Characteristics of Some Precollectors for Respirable Sampling

Name	Type	Sampling Rate (L/min)	Weight (kg)
10-mm nylon cyclone	Cyclone	1.7	0.18[a]
½-in. HASL	Cyclone	9	0.023
1-in. HASL	Cyclone	75	0.11
Uniclone 2 (Aerotec 2)	Cyclone	430	2.0
MRE gravimetric dust sampler	Elutriator	2.5	3.8[b]
Hexlet	Elutriator	50	5.0[b]
P.S. universal impactor	Impactor	6.2	0.1

[a]Includes filter holder and supporting frame.
[b]Includes pump.

to rotate around in the cyclone several times before exiting to the filter at the top center of the cyclone. During the rotation, the larger particles are deposited on walls due to their centrifugal motion. Very large particles and chunks of collected material fall to the "grit pot" at the bottom of the cyclone. Careful experimental evaluations have found that when operated at 0.10 m^3/hr [1.7 L/min], this cyclone has a collection efficiency versus aerodynamic diameter that closely matches that of the ACGIH respirable criterion. The cyclone is usually mounted with the filter in a

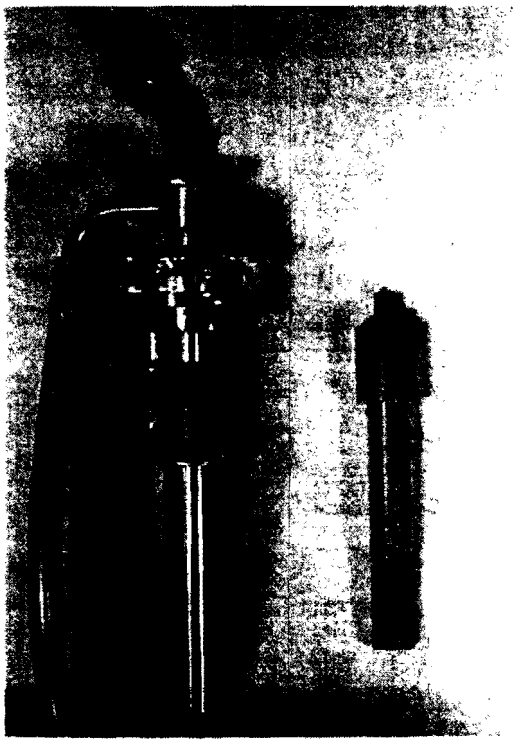

FIGURE 11.9 10-mm nylon cyclone for respirable sampling.

holder and positioned in the breathing zone of the worker whose exposure is being evaluated. The filter is connected by tubing to a battery-powered pump (see Section 10.7) worn on the worker's belt.

The horizontal elutriator shown schematically in Fig. 11.10 is designed for respirable dust sampling. The instrument is bulkier than the nylon cyclone and not suitable for personal sampling. The principle of operation of the horizontal elutriator is covered in Section 3.9. The device must be maintained in a level position during sampling.

Thoracic fraction is another size-selective sampling criterion based on regional deposition. It is defined as the fraction of ambient aerosol particles that will pass beyond the larynx and reach the thorax or chest during inhalation. Sampling in accordance with this criterion is appropriate for materials that are hazardous when deposited in the lung airways or alveolar regions. Thoracic fraction is analogous to respirable fraction, but with a cutsize (size corresponding to a thoracic fraction of 50%) of 10 μm in aerodynamic diameter (See Fig. 11.5.) The thoracic fraction, TF, is defined by the ACGIH criterion as

$$\mathrm{TF} = (\mathrm{IF})(1 - F(x')) \tag{11.15}$$

where IF is the inhalable fraction given by Eq. 11.7 and $F(x')$ is the cumulative fraction for the standardized normal variable x',

$$x' = 2.466 \ln(d_a) - 6.053 \tag{11.16}$$

in which d_a is in μm. Equation 11.12 can be used to approximate $F(x')$ by replacing x with x', as given by Eq. 11.16, throughout. A simpler expression permits the direct calculation of TF in terms of IF and d_a.

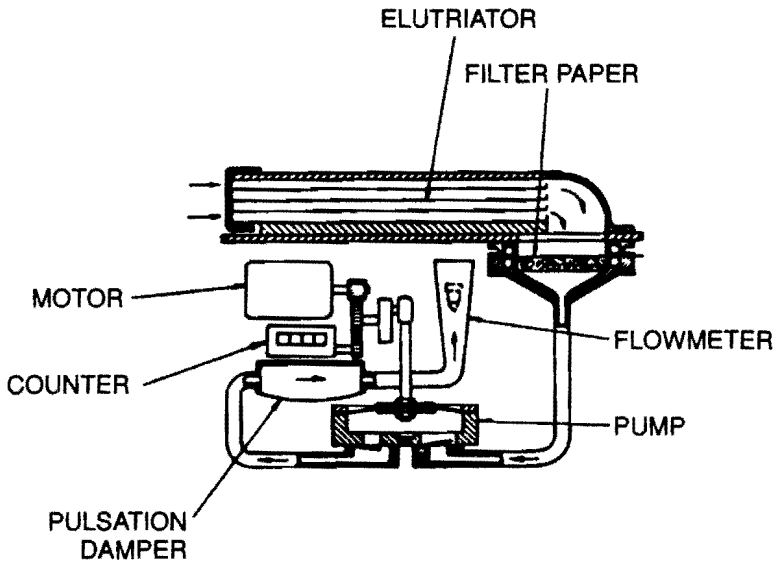

FIGURE 11.10 Schematic diagram of MRE gravimetric dust sampler. Reprinted with permission from *Air Sampling Instruments*, 5th ed., 1978, American Conference of Governmental Industrial Hygienists, 1330 Kemper Meadow Drive, Cincinnati, OH 45240.

$$TF = (IF)(1 - \exp(-\exp(2.55 - 0.249\, d_a))) \tag{11.17}$$

The thoracic fraction calculated by Eq. 11.17 differs from that calculated by Eqs. 11.15, 11.16, and 11.12 by less than 0.006 for d_a from 0 to 100 μm. The collection efficiency of a thoracic precollector CE_T is

$$CE_T(d_a) = 1 - TF(d_a) \tag{11.18}$$

Thoracic fraction samplers are reviewed by Baron and John (1999).

Closely related to the thoracic fraction criterion is the PM-10 sampling criteria promulgated by the U.S. Environmental Protection Agency in 1987 as the standard method for ambient particulate sampling. Like thoracic sampling, PM-10 sampling is based on those particles that penetrate to the thorax. The cutoff size is the same, 10 μm in aerodynamic diameter, but there are two important differences. First, PM-10 is a fraction of the total ambient particulate, not a subfraction of the inhalable particulate, as is the thoracic fraction. Second, the cutoff curve that defines PM-10 is considerably sharper than that for the thoracic fraction. The fraction of particles of diameter d_a included in the PM-10 fraction, PF_{10}, can be estimated by

$$\begin{aligned} PF_{10} &= 1.0 && \text{for } d_a < 1.5\ \mu m \\ PF_{10} &= 0.9585 - 0.00408 d_a^2 && \text{for } 1.5 < d_a < 15\ \mu m \\ PF_{10} &= 0 && \text{for } d_a > 15\ \mu m \end{aligned} \tag{11.19}$$

where d_a is in μm. PM-10 fractions calculated by Eq. 11.19 differ from those given in the [U.S.] Code of Federal Regulations (40CFR53.43, Revised July 1, 1997) by less than 0.0005. Specifications are also given for wind tunnel testing of new sampler designs and the range of wind velocities (2–24 km/hr [0.55–6.7 m/s]) over which samplers are to meet the PM-10 criteria. PM-10 samplers range from high volume samplers with flow rates of 1.13 m^3/min [1130 L/min] to low-volume dichotomous samplers with flow rates of 1.0 m^3/hr [16.7 L/min]. A PM-10 inlet for a high-volume sampler is shown in Figure 11.11. The dichotomous sampler uses a virtual impactor to cut the PM-10 particle fraction at 2.5 μm for visibility and fine-particle evaluation. Because of concern over the health effects of fine particles in the ambient environment, in 1997 the Environmental Protection Agency adopted new standards for sampling fine particles, PM-2.5. The cutoff curve for PM-2.5 is defined by an impactor cutoff curve similar to that for the virtual impactor used in the dichotomous sampler. The following empirical expression gives the fraction of particles of diameter d_a that are included in the PM-2.5 fraction, $PF_{2.5}$.

$$PF_{2.5} = [1 + \exp(3.233 d_a - 9.495)]^{-3.368} \tag{11.20}$$

where d_a is particle aerodynamic diameter in μm. PM-2.5 fractions calculated by Eq. 11.20 differ from those given in the [U.S.] Code of Federal Regulations (40CFR53.62, Revised July 18, 1997) by less than 0.001. A personal PM-10 or PM-2.5 sampler utilizing single-stage impaction is available from SKC, Inc. located in Eighty Four, PA. Other devices use cyclones or spiral inlets to achieve the 2.5 μm cutoff.

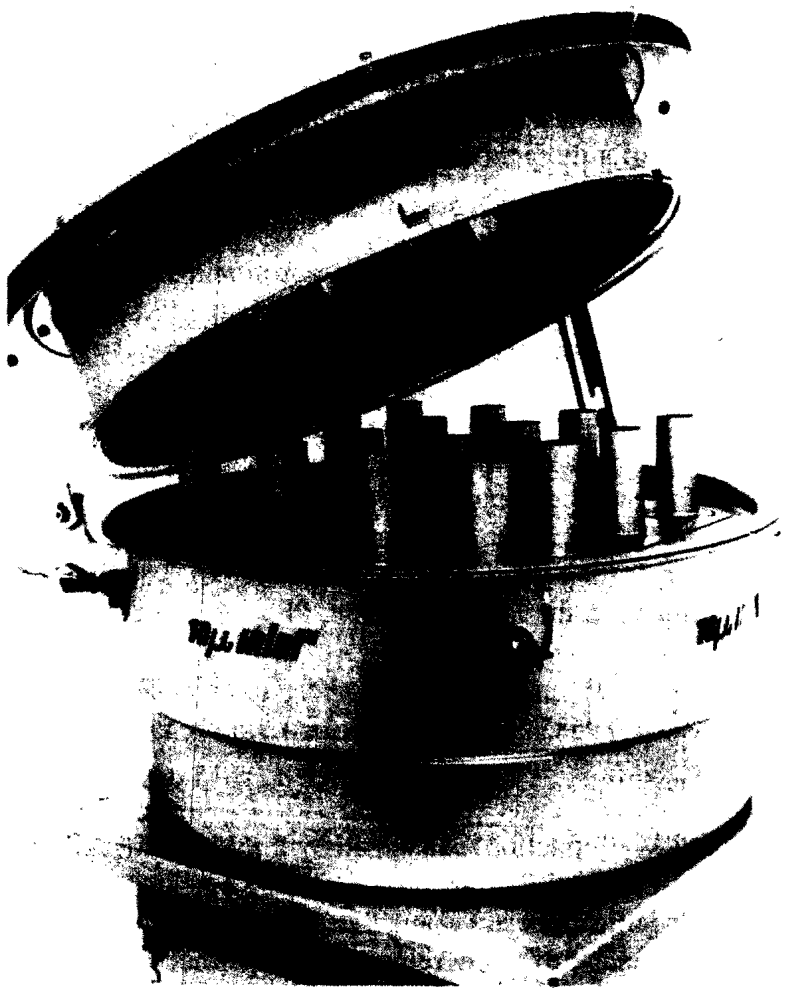

FIGURE 11.11 PM-10 inlet for a high-volume dichotomous sampler. Photo courtesy of Graseby-Andersen, Smyrna, GA.

The U.S. Occupational Safety and Health Administration (OSHA) has recommended a size-selective dust standard for evaluating the health hazards of cotton dust. The standard is based on filter samples taken using a vertical elutriator as a precollector. The elutriator is operated to remove particles larger than 15 μm in aerodynamic diameter from the aerosol stream. An epidemiological correlation has been found between the prevalence of byssinosis among cotton mill workers and the concentration of dust, as measured by the vertical elutriator method. The 15-μm cutoff size was chosen to represent the upper limit for those particles that will deposit in the *alveolar or tracheobronchial region*. Large nonrespirable fibers, called linters, clog the inlets of conventional samplers and can significantly bias mass concentration measurements.

The principle of operation of the vertical elutriator is covered in Section 3.9. The standard cotton dust vertical elutriator, shown in Fig. 11.12, is 15 cm in diameter and 70 cm high. The inlet is at the bottom, and a standard 37-mm filter holder is

FIGURE 11.12 Vertical elutriator for cotton dust sampling. Courtesy of Graseby Andersen, Inc., Smyrna, GA.

mounted at the top. The recommended flow rate of 7.4 L/min will provide an *average* upward velocity in the widest section of the elutriator of 0.68 cm/s, equal to the terminal settling velocity of a 15-μm sphere of standard density. Apparently, the conical section at the inlet was added to prevent air currents from disrupting the flow in the main section. Unfortunately, the inlet section causes a jet of air to travel along the centerline with sufficient velocity to permit particles of 30 μm in aerodynamic diameter to reach the filter. This nonuniform flow in the elutriator results in a gradual "cutoff" over a wide range in particle size. A further problem may arise because 95-μm particles can enter the inlet, but will be trapped in the elutriator's conical section and act as a floating filter for the air passing through.

PROBLEMS

11.1 According to Table 11.1, what section of the respiratory system has the highest Reynolds number, and what is the Reynolds number at an inhalation flow rate of 3.6 m^3/hr [1.0 L/s]?

ANSWER: Trachea, 4200.

11.2 What fraction of 4.0-μm particles will deposit in the head airways? Assume an average adult engaged in light work and a particle density of 1000 kg/m^3 [1.0 g/cm^3].
ANSWER: 0.82.

11.3 Using the ACGIH respirable fraction criteria, calculate (a) the fraction of *inhaled* particles with an aerodynamic diameter of 4.5 μm that reach the alveolar region and (b) the fraction of *ambient* 4.5-μm particles that reach the alveolar region.
ANSWER: 0.44, 0.39.

11.4 Calculate the inhalable and thoracic fractions for 7-μm spheres of standard density. Assume that the external air velocity is less than 4 m/s.
ANSWER: 0.83, 0.74.

11.5 On the basis of the ICRP model, estimate the fraction of 3.0-μm particles (ρ_p = 4000 kg/m^3 [4.0 g/cm^3]) that deposits in the alveolar region for an average adult.
ANSWER: 0.045.

11.6 An aerosol is composed of equal numbers of 0.02- and 2.0-μm particles. Using Fig. 11.3, estimate the fraction that will deposit in the alveolar region based on number and based on mass.
ANSWER: 0.31, 0.14.

REFERENCES

ACGIH, *1997 Threshold Limit Values and Biological Exposure Indices*, ACGIH, Cincinnati, (1997).

ACGIH Air Sampling Procedures Committee, *Particle Size-Selective Sampling in the Workplace*, American Conference of Governmental Industrial Hygienists, Cincinnati, OH (1985).

Baron, P. and John, W., "Sampling for Thoracic Aerosols," in *Particle Size-Selective Sampling for Particulate Air Contaminants*, ACGIH, Cincinnati (1999).

European Committee for Standardization (CEN), "Workplace Atmospheres—Size Fraction Definitions for Measurement of Airborne Particles," CEN Standard EN 481, Brussels: European Committee for Standardization, 1993.

Hatch, T. F., and Gross, P., *Pulmonary Deposition and Retention of Inhaled Aerosols*, Academic Press, New York, 1964.

Hinds, W. C., "Inhalable Aerosol Samplers," in *Particle Size-Selective Sampling for Particulate Air Contaminants*, ACGIH, Cincinnati (1999).

Hinds, W. C., Kennedy, N. J., and Tatyan, K., "Inhalability of Large Particles for Mouth and Nose Breathing," *J. Aerosol Sci.*, **29**, S277-S278 (1998).

International Commission on Radiological Protection, "Human Respiratory Tract Model for Radiological Protection," Annals of the ICRP, Publication 66, Elsevier Science, Inc., Tarrytown, NY (1994).

International Standards Organization, "Size Definitions for Particle Sampling: Recommendations of Ad Hoc Working Group Appointed by Committee TC 146 of the International Standards Organization," *Am. Ind. Hyg. Assoc. J.*, **42**, (5) A64–A68 (1981).

Kenny, L. C., Aitkens, R., Chalmers, C., Fabries, J. F., Gonzalez-Fernandez, E., Kronhout, H., Liden, G., Mark, D., Riediger, G., and Prodi, V., "A Collaborative European Study of Personal Inhalable Aerosol Sampler Performance," *Ann. Occup. Hyg.*, **41**, 135–153 (1997).

Lippmann, M., "Regional Deposition of Particles in the Human Respiratory Tract," in Lee, D. H. K., Falk, H. L., Murphy, S. O., and Geiger, S. R. (Eds.), *Handbook of Physiology, Reaction to Environmental Agents*, American Physiological Society, Bethesda, MD, 1977.

Lippmann, M., "Size-Selective Health Hazard Sampling," in *Air Sampling Instruments for Evaluation of Atmospheric Contaminants*, 8th ed., ACGIH, Cincinnati, 1995.

Mark, D., and Vincent, J. H., "A New Personal Sampler for Airborne Total Dust in Workplaces," *Ann. Occup. Hyg.*, **30**, 89–102 (1986).

Mark, D., Vincent, J. H., Gibson, H., and Lynch, G., "A New Static Sampler for Airborne Total Dust in Workplaces," *Am. Ind. Hyg. Assoc. J.*, **46**, 127–43 (1985).

National Council on Radiation Protection and Measurement, *Deposition, Retention and Dosimetry of Inhaled Radioactive Substances*, Report S.C. 57-2, NCRP, Bethesda, MD (1994).

Phalen, R. F., *Inhalation Studies: Foundations and Techniques*, CRC Press, Boca, Raton, FL, 1984.

Vincent, J. H., Mark, D., Miller, B. G., Armbruster, L., and Ogden, J. L., "Aerosol Inhalability at Higher Windspeeds," *J. Aerosol Sci.*, **21**, 577–586 (1990).

Vincent, J. H., *Aerosol Sampling: Science and Practice*, Wiley, Chichester, U.K., 1989.

Walton, W. H., *Inhaled Particles*, vol. 4, Pergamon, Oxford, 1977.

Werner, M.A., Spear, T. M., and Vincent, J. H., "Investigation into the Impact of Introducing Workplace Aerosol Standards Based on the Inhalable Fraction," *Analyst*, **121**, 1207–1214 (1996).

Yeh, H. C. and Schum, G. M., "Models for Human Lung Airways and their Application to Inhaled Particle Deposition," *Bull. Math. Biology*, **42**, 461–480 (1980).

Yeh, H. C. Cuddihy, R. G., Phalen, R. F., and Chang, I-Y., "Comparisons of Calculated Respiratory Tract Deposition of Particles Based on the Proposed NCRP Model and the New ICRP Model," *Aerosol Sci. Tech.*, **25**, 134–140 (1996).